

Friction at the Contact Between Bearing Balls and Cotton-Phenolic Cage Material

10 June 2004

Prepared by

P. A. BERTRAND
Space Materials Laboratory
Laboratory Operations

Prepared for

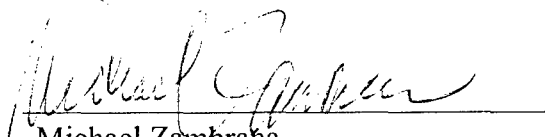
SPACE AND MISSILE SYSTEMS CENTER
AIR FORCE SPACE COMMAND
2430 E. El Segundo Boulevard
Los Angeles Air Force Base, CA 90245

Engineering and Technology Group

This report was submitted by The Aerospace Corporation, El Segundo, CA 90245-4691, under Contract No. FA8802-04-C-0001 with the Space and Missile Systems Center, 2430 E. El Segundo Blvd., Los Angeles Air Force Base, CA 90245. It was reviewed and approved for The Aerospace Corporation by P. D. Fleischauer, Principal Director, Space Materials Laboratory. Michael Zambrana was the project officer for the Mission-Oriented Investigation and Experimentation (MOIE) program. -

This report has been reviewed by the Public Affairs Office (PAS) and is releasable to the National Technical Information Service (NTIS). At NTIS, it will be available to the general public, including foreign nationals.

This technical report has been reviewed and is approved for publication. Publication of this report does not constitute Air Force approval of the report's findings or conclusions. It is published only for the exchange and stimulation of ideas.



Michael Zambrana
SMC/AXE

REPORT DOCUMENTATION PAGE				Form Approved OMB No. 0704-0188	
<small>Public reporting burden for this collection of information is estimated to average 1 hour per response, including the time for reviewing instructions, searching existing data sources, gathering and maintaining the data needed, and completing and reviewing this collection of information. Send comments regarding this burden estimate or any other aspect of this collection of information, including suggestions for reducing this burden to Department of Defense, Washington Headquarters Services, Directorate for Information Operations and Reports (0704-0188), 1215 Jefferson Davis Highway, Suite 1204, Arlington, VA 22202-4302. Respondents should be aware that notwithstanding any other provision of law, no person shall be subject to any penalty for failing to comply with a collection of information if it does not display a currently valid OMB control number. PLEASE DO NOT RETURN YOUR FORM TO THE ABOVE ADDRESS.</small>					
1. REPORT DATE (DD-MM-YYYY) 10-06-2004		2. REPORT TYPE		3. DATES COVERED (From - To)	
4. TITLE AND SUBTITLE Friction at the Contact Between Bearing Balls and Cotton-Phenolic Cage Material				5a. CONTRACT NUMBER FA8802-04-C-0001	
				5b. GRANT NUMBER	
				5c. PROGRAM ELEMENT NUMBER	
6. AUTHOR(S) P. A. Bertrand				5d. PROJECT NUMBER	
				5e. TASK NUMBER	
				5f. WORK UNIT NUMBER	
7. PERFORMING ORGANIZATION NAME(S) AND ADDRESS(ES) The Aerospace Corporation Laboratory Operations El Segundo, CA 90245-4691				8. PERFORMING ORGANIZATION REPORT NUMBER TR-2004(8565)-3	
9. SPONSORING / MONITORING AGENCY NAME(S) AND ADDRESS(ES) Space and Missile Systems Center Air Force Space Command 2450 E. El Segundo Blvd. Los Angeles Air Force Base, CA 90245				10. SPONSOR/MONITOR'S ACRONYM(S) SMC	
				11. SPONSOR/MONITOR'S REPORT NUMBER(S) SMC-TR-04-15	
12. DISTRIBUTION/AVAILABILITY STATEMENT Approved for public release; distribution unlimited.					
13. SUPPLEMENTARY NOTES					
14. ABSTRACT Current analytical models of ball-bearing behavior generally use values of cage (also called ball separator or ball retainer) friction that do not accurately reflect the dependence of cage friction on the lubrication regime at the cage interfaces (boundary, mixed, or hydrodynamic; starved or fully flooded), ball speed, lubricant identity, ball material and cage material, or they use values that are essentially adjustable parameters. This work reports measurements of coefficient of friction (COF) for balls of three different materials against flats of cotton-phenolic retainer material using three different oils. COFs were measured at 200 g load and sliding speeds between 0.007 and 9.7 m/s. Steel, silicon nitride, and TiC-coated steel balls were used; a mineral oil, a poly- α -olefin, and a trialkylated cyclopentane of the same viscosity were used as lubricants. The complex variation of COF with experimental conditions is related to current theories of lubricant behavior. The data are provided in an appendix for use in modeling programs.					
15. SUBJECT TERMS Friction, Lubricating oils, Cotton-phenolic composite					
16. SECURITY CLASSIFICATION OF:			17. LIMITATION OF ABSTRACT	18. NUMBER OF PAGES 24	19a. NAME OF RESPONSIBLE PERSON Ann Bertrand
a. REPORT UNCLASSIFIED	b. ABSTRACT UNCLASSIFIED	c. THIS PAGE UNCLASSIFIED			19b. TELEPHONE NUMBER (include area code) (310)336-6297

Acknowledgments

The author thanks Dr. P. P. Frantz for helpful discussions about ball bearing models, Mr. K. K. Lue and Mr. J. J. Kirsch for designing and building the test fixture, Dr. O. Esquivel for performing the temperature measurements, and Dr. W. R. Jones, Jr. of NASA Glenn Research Center for supplying the TiC-coated ball.

Contents

1. Introduction.....	1
2. Experimental	3
2.1 Test Fixture.....	3
2.2 Materials	3
2.3 Procedure.....	4
2.4 Temperature Measurement	5
3. Results and Discussion	7
3.1 Mixed Regime	8
3.2 Hydrodynamic Regime	11
3.3 High-Speed Regime	13
4. Summary and Conclusions	17
References	19
Appendix — COF Data	21

Figures

1. Coefficient of friction fixture.....	3
2. COF of cotton-phenolic against large steel ball for poly- α -olefin oil	8
3. COF of cotton-phenolic against silicon nitride ball for poly- α -olefin oil	9
4. COF of cotton-phenolic in the mixed lubrication regime for poly- α -olefin oil	9
5. COF of cotton-phenolic against large and small steel balls for synthetic oils.....	10
6. COF of cotton-phenolic against steel, silicon nitride and TiC-coated balls in the hydrodynamic regime.....	11
7. COF of cotton-phenolic against balls for petroleum and synthetic oils	12

8. Fit of COF to square root of speed in hydrodynamic region	13
--	----

Tables

1. Oil Properties	4
2. Oil on Balls, Well-Lubricated Tests	7
3. COF in High-Speed Regime.....	14

1. Introduction

Analytical models of ball bearing operation, such as the well-known program ADORE by P. Gupta and DYBA by A. Leveille, are increasingly used to predict the performance characteristics and guide the design of mechanical systems incorporating ball bearings. Much is understood about the rolling contact between the ball and the raceway. However, precise knowledge of the ball-cage and cage-land contacts is lacking. When the load on an angular contact bearing becomes asymmetric, or when the preload on the bearing is insufficient to overcome the gyroscopic moment of the spinning balls, the resulting loads at the ball-cage and cage-land interfaces may grow to many times their normal values. Under these conditions, predictions of bearing torque and wear rates become sensitively dependent on the friction coefficients at these interfaces. Furthermore, high friction at the ball-cage and cage-land interfaces of ball bearings can cause retainer instability, a life-limiting vibration that eventually results in fracture of the retainer. Models attempt to include the interactions, generally in a semiempirical manner, and the model predictions can be sensitive to cage interactions included in this way. But the models may not use the most accurate values of cage friction: generally they use values that do not accurately reflect the dependence of cage friction on the lubrication regime at the cage interfaces (boundary, mixed, or hydrodynamic; starved or fully flooded), ball speed, lubricant identity, ball material and cage (retainer) material, or they use values that are essentially only adjustable parameters.

This work reports measurements of coefficient of friction (COF) for three different ball materials against cotton-phenolic retainer material. Balls of two different diameters were used. Three oils (two synthetic oils and one mineral oil), all chosen as of interest to spacecraft systems, were used as lubricants. The experiments were conducted on a ball-on-flat test fixture in which the contact was 100% sliding, as are the ball-cage and cage-land contacts in a ball bearing. There is no provision for intermittent contact in the experiment, although in a ball bearing, contact between the cage and the metal parts is probably intermittent. Sliding speeds were varied between 0.007 and 9.7 m/s, load was held constant at 200 g force (chosen for a specific spacecraft application). COF can vary by a factor of 10 over the speed range investigated, showing how important it is to select appropriate COF values for use in modeling ball bearing behavior.

2. Experimental

2.1 Test Fixture

The tests were carried out in air on a ball-on-flat fixture, shown in Figure 1. The ball is attached to one of two motors for either low-speed (less than 1500 rpm) or high-speed (between 5200 and 7500 rpm) operation. The load force and the reaction force perpendicular to the load force are measured by a digital voltmeter via proximeters that are calibrated before each day's experiments. The proximeters and the sample flat holder are fixed to a microscope stage that is moved by a micrometer to contact the flat with the ball at the desired force. The balls are not perfectly centered on the rotation axis of the motor, leading to some degree of run-out that is different for each ball and each experiment. On our previous apparatus,¹ the force measurements were routed to a computer, and it was possible to examine the effects of runout on the measurements directly. This feature has not yet been implemented on the current fixture.

2.2 Materials

Two steel balls, a silicon-nitride ball, and a TiC-coated steel ball were used in the tests. The steel balls have a surface roughness R_a of $0.020\text{ }\mu\text{m}$, and are made of 440C steel. One is 0.5 in. (1.27 cm) in diameter while the other is 0.875 in. (2.22 cm) in diameter. The silicon-nitride ball, which is 0.875 in. (2.22 cm) in diameter, has a surface roughness R_a of $0.007\text{ }\mu\text{m}$, and is made of NBD 200 silicon nitride with a magnesia sintering aid. The TiC-coated steel ball, which is 0.5 in. (1.27 cm) in diameter, was made by CSEM and has a surface roughness R_a of $0.015\text{ }\mu\text{m}$.

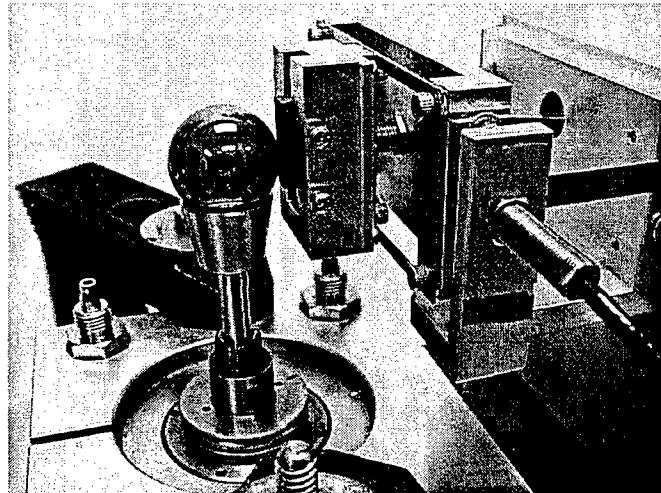
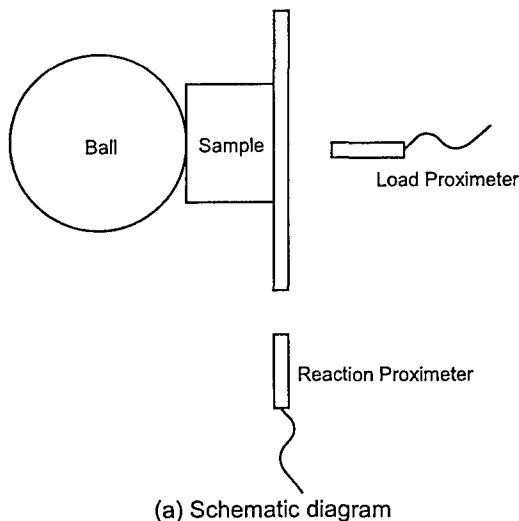


Figure 1. Coefficient of friction fixture.

The flats were cotton-phenolic composite. They were soxhlet-extracted overnight in heptane, baked overnight in vacuum at 110°C, and placed immediately into oil baths that were maintained in desiccators. They remained submerged in oil at least one month prior to their first use, and were kept in the oil baths in the desiccators during the years over which these tests were conducted. The surface used was typical of the ball-pocket or retainer-land interface of a ball bearing retainer: the plane of the cotton cloth is perpendicular to the surface, so cut threads are present at the surface. The threads do not extend above the surface, and may be recessed. The surface roughness R_a of the composite is 1–2 μm , with large dips every several hundred μm due to the threads.

Three formulated oils in use in the spacecraft industry were examined. Nye 2001® is a trialkylated cyclopentane commonly called "Pennzane®," formulated with a mixture of aryl phosphate esters. Nye 188B® is a poly- α -olefin, also formulated with the same mixture of aryl phosphate esters. These formulated oils were obtained from Nye Lubricants. A mineral oil, Apiezon C®, was obtained from Apiezon Products and formulated in-house with the same additive as the two synthetic oils. Some properties of the oils are listed in Table 1. Baths of each oil were kept in desiccators, and the test blocks were stored in them. Oil to lubricate the balls was withdrawn from the same baths of dry oil.

Table 1. Oil Properties

Property	Apiezon C	Nye 188B	Nye 2001
Density (g/cm ³) @ 20°C	0.87	0.85	0.85
Viscosity (cSt) @ 40°C	90	107	107
@ 100°C	10.6	14.5	14.3

2.3 Procedure

The proximeters were calibrated each day before tests were begun, using dead weights. A sample flat was removed from its oil bath, and wiped with a lint-free cloth to remove excess oil. There is still some oil present on the surface after this treatment. For experiments under "well-lubricated" conditions, the flat was used directly. For experiments under "poorly lubricated" conditions, the flat was wrapped in a lint-free cloth and centrifuged at 2000 rpm (850 G) for 15 min to remove the surface oil. The block was then inserted into the test fixture.

A ball was cleaned by wiping with a lint-free cloth saturated with heptane, then attached to one of the two motors. For "well-lubricated" conditions, oil was added by pipette to the surface of the ball (10 μl for the large balls, and 3 μl for the small balls). The ball was then rotated for 1 min at 1500 rpm for the low-speed motor or 7650 rpm for the high-speed motor. The speed was lowered to 200 or 5100 rpm, and the block was moved into contact with the rotating ball until the load proximeter read the desired value. A single load, 200 g force (2 N), was used for all the tests, as discussed below. Then the ball speed was increased to 1500 or 7650 rpm for 1 min before the tests began. For "poorly lubricated" conditions, no oil was added to the ball. The ball was rotated at 200 or 5100 rpm as the load was set, then the speed was increased to 1500 or 7650 rpm for 1 min before the tests began. This procedure ensured a consistent amount of oil for each experiment, as will be shown below.

Data were collected at a variety of speeds in random order, with both clockwise and counterclockwise directions of ball rotation. Under well-lubricated conditions a meniscus of oil with a diameter of about 1 to 2 mm was clearly visible at the contact, and when the motor was stopped, swirls of inter-

ference colors appeared on the ball due to the thin oil film. Neither meniscus nor interference colors were observed during poorly lubricated experiments. The data reported are averages of at least four measurements at each speed. The flats were typically exposed to air for less than 3 h, so displacement of oil from the cotton-phenolic composite by moisture from the air was not expected to be a problem.²

After a set of experiments, the ball was removed from the fixture, and the oil was rinsed off into a preweighed beaker using heptane. The heptane was evaporated, and the beaker was weighed to determine the amount of oil that had been on the ball.

2.4 Temperature Measurement

The temperature near the ball-flat contact was measured during rotation for two experiments using the large steel ball and poly- α -olefin oil, one at 1.8 m/s (1500 rpm) and one at 9 m/s (7500 rpm). An AGEMA Thermovision 570 infrared camera with a room-temperature bolometer detector that senses in the 8–13 μm wavelength range was used to monitor the temperature during the experiments, and a small thermocouple was squeezed between the (static) ball and the flat after each experiment to verify the calibration of the camera.

3. Results and Discussion

A single-load, 2 N, was used for all the experiments. This load was chosen originally to simulate the load expected at the ball-cage interface for a specific spacecraft application. Variation of load over a wide range was not attempted in these tests, although some (less than 10%) variation was present between different tests. Since the load was constant, the Hertzian stress at the ball-flat contact was higher for the small balls than the large balls (99 MPa and 66 Mpa, respectively). Real ball-cage and cage-land contacts are probably intermittent, with load varying over short periods of time; this phenomenon was not studied in these experiments.

The weight of oil remaining on a ball after a set of experiments was measured, and the thickness of the oil film on the ball was calculated assuming the film was continuous and even (Table 2). This thickness is only approximate since the films may not be continuous or even: when the ball is stopped after high-speed experiments, for instance, we observe interference colors, which indicate some variation of film thickness. The estimated thickness of oil on the small balls (steel and TiC-coated) is the same as on the large balls (steel and silicon nitride) for the well-lubricated, low-speed tests. The weight of oil found on the balls and the estimated oil thickness for the well-lubricated, high-speed tests are lower than for the low-speed tests, although the same volume of oil was applied to the ball initially. This is most likely due to the larger centrifugal force on the surface of the balls at high rotation rate driving the oil off the balls. In addition, the estimated thickness for the large balls is lower than for the small balls at high speed, probably also due to higher centrifugal force at the surface of the large balls compared to the small balls. No measurable oil was found on the balls after tests under poorly lubricated conditions.

The λ ratio, the ratio of oil film thickness to composite surface roughness, is often used as a general guide to the type of lubrication (mixed or full-film) present in a bearing. For λ greater than about 3, it is generally considered that the surfaces are fully separated, while for λ less than 1, there is much contact between the surfaces. The film thickness that should be used when calculating λ is that entrained between the surfaces by the movement of the parts. This will be discussed in more detail below, but we can make an initial estimate of λ from the amount of oil available. Using this approximation, the well lubricated tests at low speed have λ of about 3–7, which implies that good separation of the contacting surfaces could occur if the oil film actually entrained between the surfaces is truly 7 μm thick. At high speed, however, λ is probably less than 1 for the large balls, and less than 2 for the small ones, implying that direct contact between the surfaces is probably inevitable.

Table 2. Oil on Balls, Well-Lubricated Tests

Test Conditions	Oil Weight (g)	Oil Film Thickness (μm)
Low speed, large balls	10 ± 2	7 ± 1
Low speed, small balls	3 ± 1	7 ± 1
High speed, large balls	1.5 ± 0.4	1.1 ± 0.3
High speed, small balls	0.8 ± 0.5	2 ± 1

As mentioned above, at least four measurements of COF were averaged for each of the reported data points. Using pooled analysis of variance, we estimate an error of ± 0.009 for the individual COFs reported.

The variation of COF with sliding speed is shown in Figure 2 for poly- α -olefin oil and the large steel ball. (The average COFs of all the ball, oil, and speed combinations are listed in the appendix.) The form of the curve for the well-lubricated experiment is often called "Stribeck-like" since it was presented by R. Stribeck in an early study of journal bearings.³ At close to zero speed, below the speeds we could reach in this study, there is boundary lubrication with a high COF, in which the surfaces contact directly and no significant lubrication by an oil film occurs. At higher speeds (below about 0.2 m/s here), the contact is in the mixed lubrication regime, with boundary friction at contacting asperities, and fluid shear in other regions. Eventually, as the oil film gets thicker and more prevalent, the shear of the oil film becomes more important, in what is termed the hydrodynamic regime. This occurs between about 0.2 and 1 m/s in the figure. Our experiments extend to even higher speeds, and we reach a region where the COF no longer increases with speed, which we will refer to as the high-speed regime. Each of these regions will be discussed in detail below.

The poorly lubricated conditions do not show a drop of COF with speed, since there is essentially no oil to be drawn into the contact to separate the surfaces. The friction increases as the speed increases, until it plateaus at high speed.

3.1 Mixed Regime

In the mixed lubrication regime, COF is dependent upon the ball material and the precise amount of oil, as well as the contact speed. Figure 3 shows the COF for the silicon-nitride ball with four different amounts of poly- α -olefin oil. All four curves extrapolate to a COF of about 0.08 at zero speed. This is not the true boundary friction of silicon nitride against clean cotton-phenolic composite because there is at least a very small amount of oil present in each of these experiments. The lowest curve was obtained in well-lubricated conditions, the middle two curves were obtained in two different poorly lubricated tests, and the upper curve was obtained after additional centrifugation of the cotton-phenolic to remove even more oil from the surface. It is clear that the exact amount of oil in

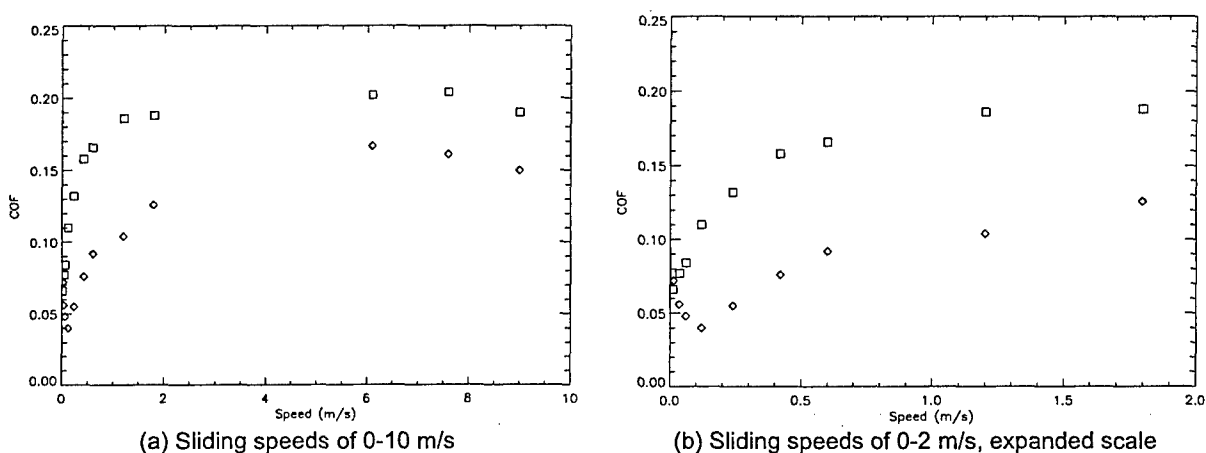


Figure 2. COF of cotton-phenolic against large steel ball for poly- α -olefin oil. ◇ represents well lubricated conditions, □ represents poorly lubricated conditions.

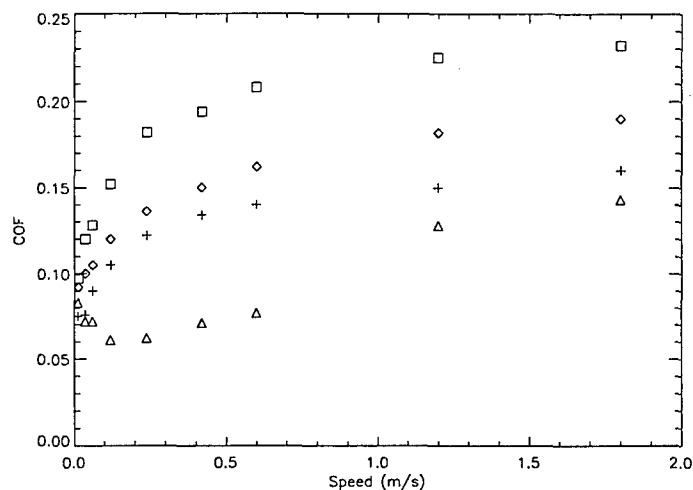


Figure 3. COF of cotton-phenolic against silicon nitride ball for poly- α -olefin oil. Δ represents well lubricated conditions, + and \diamond represent two cases of poorly lubricated conditions, and \square represents even further oil-depleted cotton-phenolic.

the contact plays a major role in determining the COF. For a silicon-nitride ball (and any of the oils studied here) at a speed of 0.1 m/s, the COF of a well-lubricated contact is about 0.07, while that of a poorly lubricated contact can be up to 0.16.

The ball material influences the COF in the mixed lubrication regime also, as can be seen in Figure 4. The two steel balls have the lowest COF at sliding speeds less than 0.1 m/s. The COF of the silicon-nitride ball is higher, and that of the TiC-coated ball is highest. One possible explanation of this behavior is the action of the phosphate ester additive; perhaps on some surfaces the additive segregates to the surface region or reacts to produce a lower (or higher) COF. However, although silicon-

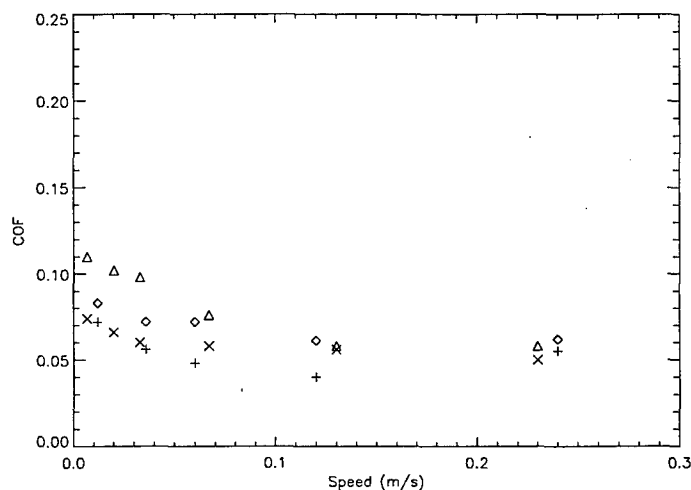


Figure 4. COF of cotton-phenolic in the mixed lubrication regime for poly- α -olefin oil. + represents the large steel ball, X represents the small steel ball, Δ represents the TiC-coated ball, \diamond represents the silicon nitride ball.

nitride surfaces do not react with aryl phosphate ester additives, steel and TiC surfaces both do, so this hypothesis cannot explain the hierarchy we observe. It is conceivable that the surface reaction products on steel and TiC have different properties, those on steel producing lower friction than a silicon-nitride surface and those on TiC producing higher friction than a silicon-nitride surface. However, preliminary measurements using unformulated oils suggest that the same hierarchy of COF obtains even in the absence of aryl phosphate ester additives. Another possible explanation is that higher COF in this region is caused by higher surface roughness, and thus more asperity contact. This hypothesis also does not explain the data: the TiC-coated ball has the same surface roughness as the steel ball, and the silicon-nitride ball is smoother. At the present time, we do not have a detailed explanation for the COF hierarchy found in these studies.

The COF for Nye 2001 and the large steel ball is unexpectedly low in the region between 0.01 and 0.3 m/s. In Figure 4, we can see that the COF for the poly- α -olefin oil is the same for the large and small steel balls. Figure 5 shows that while the COF for the trialkylated cyclopentane oil for the small ball is the same as that for the poly- α -olefin oil; for the large ball it is much lower. It is possible, but unlikely, that the measurements are statistically anomalous since each point is the average of at least four measurements taken on several separately prepared samples on occasions that were weeks apart. Another possibility is a systematic error that obtains for only this combination of oil and ball; we have not yet identified such an error. A third possibility is that the data are accurate, and there is a difference in the behavior of the trialkylated cyclopentane oil with phosphate additives on the large and small balls. At present, the only parameter we know to be different in the two cases is the Hertzian stress (66 MPa for the large ball and 99 MPa for the small ball). Unformulated trialkylated cyclopentane oil does not show any unexpected changes in flow properties for pressures ranging from 0.5 to 1.8 GPa and speeds of 0.01 to 1.0 m/s.^{4, 5} To our knowledge, no similar experiments have been

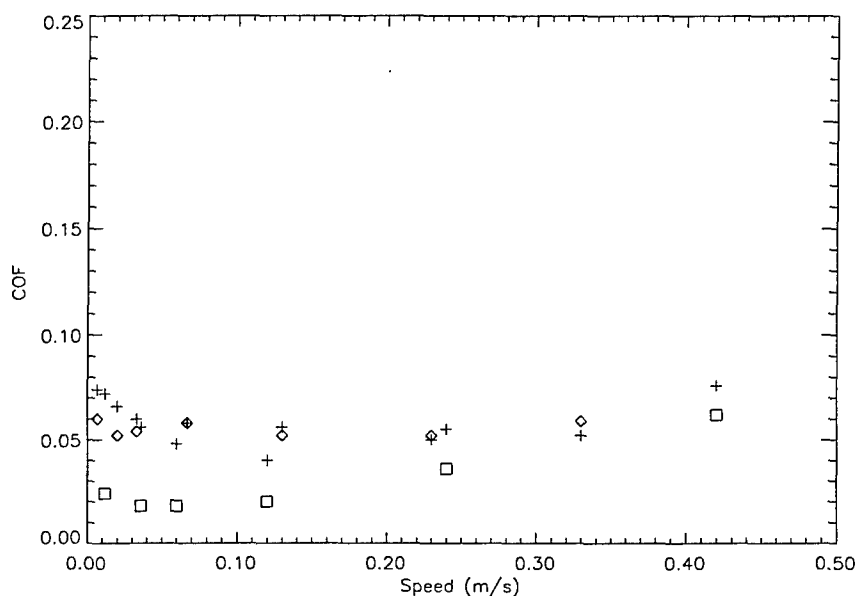


Figure 5. COF of cotton-phenolic against large and small steel balls for synthetic oils. + represents poly- α -olefin oil and both large and small balls, ◇ represents trialkylated cyclopentane oil and the small ball, □ represents trialkylated cyclopentane oil and the large ball.

performed for the formulated oil at pressures as low as 66 MPa. We can speculate that at low pressure the flow of additive and oil molecules is not greatly influenced by pressure, while at higher pressure there is an effect; however, even 99 MPa is a very low pressure for any modification of flow properties.

3.2 Hydrodynamic Regime

In Figures 4 and 5, it is noticeable that starting between 0.1 and 0.2 m/s, the COFs of all the surfaces begin to coalesce. Figure 6 shows this phenomenon for both the poly- α -olefin oil and the trialkylated cyclopentane oil, and all four surfaces: the contribution of the surfaces becomes less important as the speed rises and more oil is entrained into the contact. The conditions of these tests are isoviscous-elastic:⁶ the load is low enough that the change in viscosity with load is unimportant (isoviscous), and the surfaces experience elastic deformation. The maximum Hertzian stress at the contact is 66 MPa, and the contact radius is 120 μm for the large balls. These values are 99 MPa and 98 μm for the small balls.

For hydrodynamic contacts, the COF is given by

$$COF = \xi \sqrt{\frac{u\eta}{P}}, \quad (1)$$

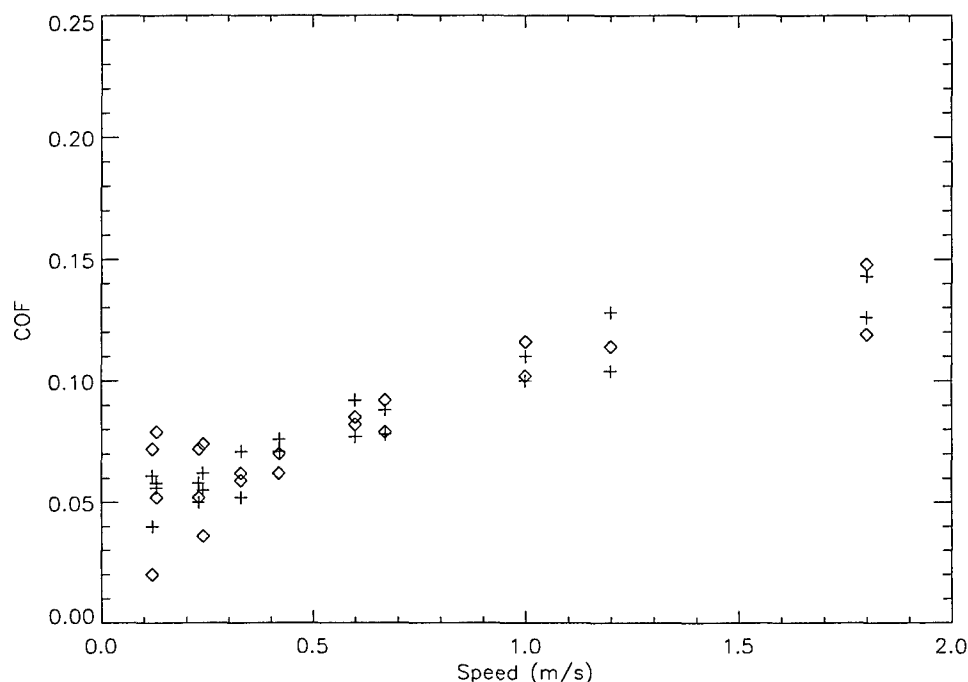


Figure 6. COF of cotton-phenolic against steel, silicon nitride and TiC-coated balls in the hydrodynamic regime. + represents poly- α -olefin oil, \diamond represents trialkylated cyclopentane oil. (For clarity, the different surfaces are not distinguished symbolically in the figure.)

where u is the sliding speed (in m/s), η is the viscosity of the fluid (in Pa s), P is the load (in N), and ζ is a parameter with dimension $[\text{length}^{-1/2}]$ ($\text{m}^{-1/2}$ in the units used here) determined by the contact geometry and the boundary conditions chosen when integrating the Reynold's equation.⁷ Equation 1 has been obtained from the Reynold's equation analytically for the cylinder-on-flat contact geometry and various boundary conditions. The effect of boundary condition on COF is marked: ζ for a zero-reverse-flow condition (typical of a contact initially charged with a fixed amount of lubricant, as in our experiments) is 8 times higher than for a fully flooded condition.⁸ Equation 1 has not been obtained analytically for the sphere-on-flat geometry to our knowledge. Some numerical solutions have been reported for specific conditions, at much higher loads (1.7 GPa contact stress)⁹ than the tests described here.

The viscosity of all three oils used in these experiments is about the same, as are the load, contact geometry, and the boundary conditions. Thus, we would expect that a plot of COF vs. u would be a single curve for all of the oils studied. However, as shown in Figure 7, the two synthetic oils have lower COF throughout the hydrodynamic region than does the mineral oil. The difference in friction of oils with the same viscosity is historically termed "oiliness,"¹⁰ and has been and continues to be a subject of much theoretical and experimental interest. The effects of pressure, film thickness, lubricant molecular size, chemistry and structure, surface chemistry, and surface roughness on lubricant rheology are being investigated by many groups (for instance, see References 11–15).

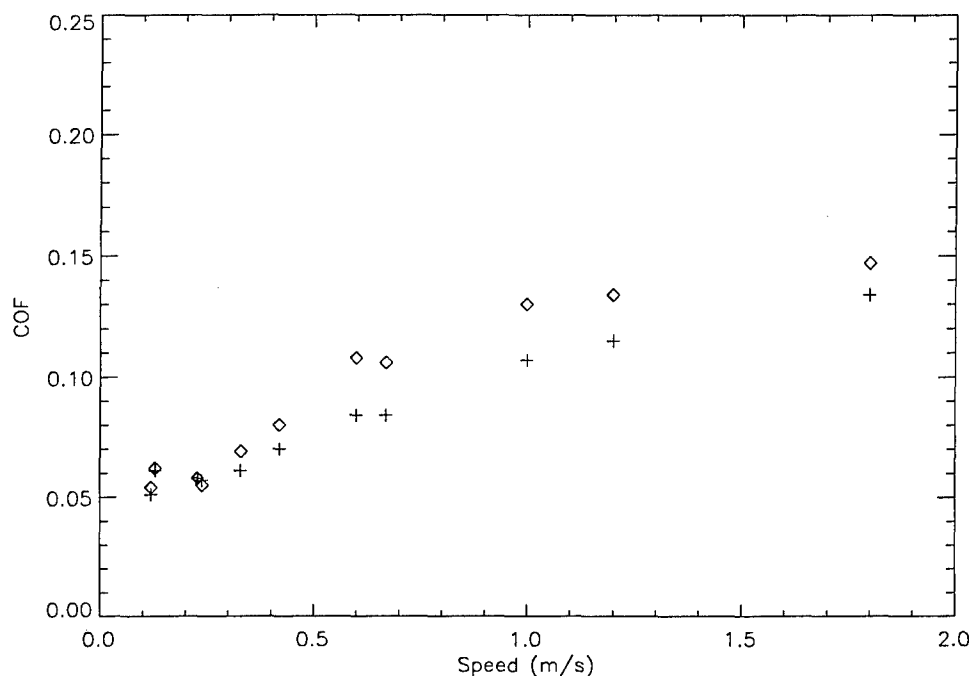


Figure 7. COF of cotton-phenolic against balls for petroleum and synthetic oils. $+$ represents the average of poly- α -olefin and trialkylated cyclopentane synthetic oils (for large and small steel, silicon nitride and TiC-coated balls), \diamond represents petroleum oil (for the same 4 balls).

Figure 8 illustrates least-squares fits of Eq. (1) to our data, constraining the lines to pass through the origin. The fits are very good for both the synthetic oils and the mineral oil; the constant of proportionality ξ is $0.306 \text{ m}^{1/2}$ for the synthetic oils and $0.370 \text{ m}^{1/2}$ for the mineral oil.

Earlier in this report, we used the amount of free oil on the ball to estimate the oil film thickness in the contact for the purpose of calculating the λ ratio. The minimum film thickness in the contact between a sphere and a flat can be calculated for fully flooded conditions, and is in the range 0.2 to $1 \text{ }\mu\text{m}$ for the load and speeds used here. However, films in starved conditions (zero-reverse-flow) are thinner than in fully flooded contacts, and, in addition, experimental evidence shows that films in sliding contacts (such as those in our experiments) are thinner than those in rolling contacts at similar speeds.¹⁶ Thus, the films in our experiments are probably always less than $1 \text{ }\mu\text{m}$ thick between the ball and the flat, leading to λ ratios of less than 1, and probable asperity contacts. The presence of asperity contacts is probably one reason why the COF of our cage-ball interface in the hydrodynamic region is higher than that measured for EHD rolling contacts of (much smoother) interfaces between balls and raceways where λ is generally greater than 3.

3.3 High-Speed Regime

As the contact speed increases above about 1 m/s in these experiments, the COF no longer increases (Figure 2). This effect has been seen in previous experiments using sliding or rolling contacts,^{8,17,18,19} and has been attributed to various combinations of thermal effects, lubricant starvation, and slip of the lubricant at the solid surfaces.

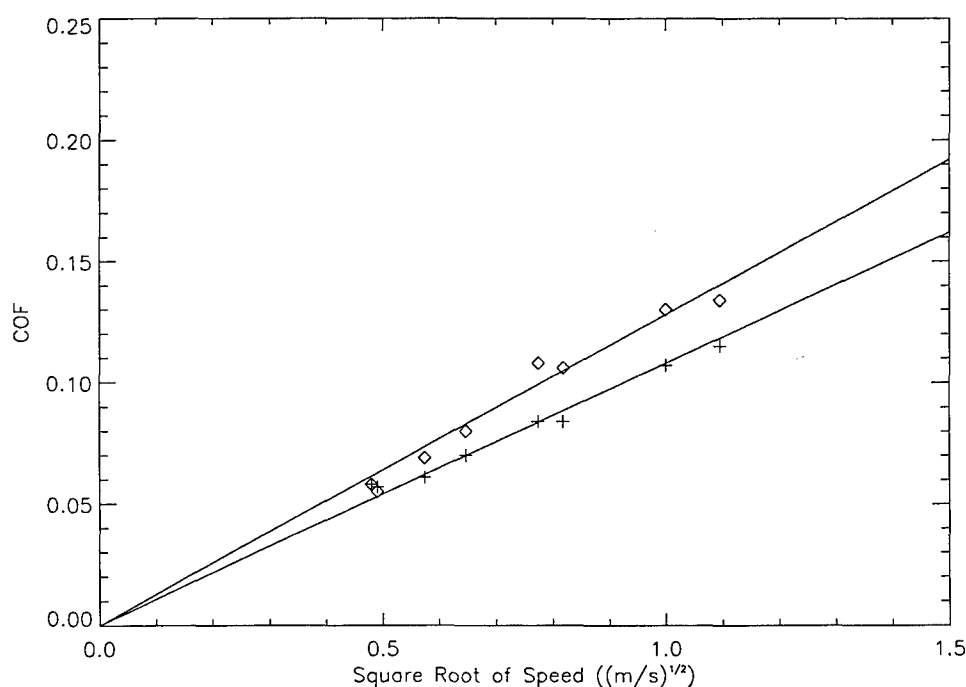


Figure 8. Fit of COF to square root of speed in hydrodynamic region. + represents all balls and both synthetic oils, ◇ represents all balls and the petroleum oil, lines are the least-squares fits to the data.

Heating at the contact occurs in our experiments. The temperature was measured for two experiments using the large steel ball. The temperature at 1.8 m/s was 25°C, and that at 9 m/s was 41°C (room temperature was 21°C). These are probably lower than the true temperature within the contact during operation. The contact region is not directly visible to the infrared camera, and although the region we observe is very close to the contact, it is probably slightly lower in temperature. The thermocouple measurements that confirm the camera measurements were taken 15 to 30 s after rotation was stopped, and the temperature has probably decreased slightly in that time period. In Table 3, we present the predicted COF for two cases: one case in which we assume that the oil is not heated above room temperature, and another case in which we assume that the oil is heated to the temperature observed by the infrared camera, taking into account the dependence of oil viscosity on temperature. The elevated temperature COF value is much closer to the measured value than is the room-temperature value. We can also predict what the temperature of the contact must be if the entire cause of the reduction of COF below the room-temperature prediction is due to thermal effects; this is listed in the table also. These temperatures (24°C at 1.8 m/s and 56°C at 9.0 m/s) are not outside the realm of possibility. Thus, heating in the contact can account for most if not all of the observation that the COF does not increase as quickly as predicted by Eq. (1) for a room-temperature contact.

Lubricant starvation can also cause COF to be lower than in a fully flooded contact. A thinner film will have less viscous drag, leading to a lower COF. As speed increases, the inlet zone for the oil into the contact moves further away from the center of the contact.^{6,19} If the contact is not fully flooded but is initially charged with oil that is present only as a meniscus around the contact (as in our experiments), eventually the inlet zone will be outside the meniscus of oil present. Above this speed, insufficient oil is present to be entrained into the contact, leading to thinner films than in a fully flooded contact at the same speed.¹⁹ The contacts in these experiments are probably starved, particularly at high speeds. The exact effect of starvation on the COF is complicated by the effects of asperity contacts, particularly with a surface as rough as that of cotton-phenolic. Models of elastohydrodynamic contacts have begun to address these questions, but for contacts under very different operating conditions than those in these experiments.⁹

A third possibility for lower COF at high speed than predicted by room-temperature, fully flooded conditions is slip between the lubricant and the surface. When solving the Reynold's equation, one component of the boundary conditions is usually the "no-slip" condition, in which the oil at the surface is assumed to travel at the speed of the surface, and all the shear takes place within the oil and none between the surface and the oil. This boundary condition fails in certain cases, such as for flow of a coarse powder across a smooth surface, and flow of liquids whose molecules are of a size comparable to the surface roughness.²⁰ If the thickness of the fluid layer and the height of the asperities are

Table 3. COF in High-Speed Regime

Speed (m/s)	COF			T (°C)	
	Estimated, no heating in contact	Estimated, with heating in contact	Measured	Measured	Estimated from measured COF*
1.8	0.145	0.130	0.134	25	24
9.0	0.325	0.189	0.141	41	56

*Estimate based on Equation (1), assuming that only thermal effects lower COF from room-temperature prediction.

both large compared to the size of the molecules (as is the case in most ball bearings), the no-slip boundary condition is generally believed to prevail even if slip actually does occur on a microscopic level.²¹ However, in a study of sliding contact between a cylinder and a flat, it has been suggested that the measured COF at high speed is lower than predicted by Eq. (1) because of failure of the no-slip boundary condition.⁸ The authors of this work did not take heating of the oil in the contact into account since they measured no temperature increase on the cylinder at a point $3/4$ of a revolution away from the contact. This is probably not the most representative contact temperature measurement, and at this point in time, we do not consider the presence of slip proven.

4. Summary and Conclusions

The COF of contacts between flats of cotton-phenolic ball bearing retainer material and bearing balls were measured at 200 g load and sliding speeds between 0.007 and 9.7 m/s. Balls of 440C steel, silicon nitride, and TiC-coated steel were used; three oils of the same viscosity (a mineral oil, a poly- α -olefin, and a trialkylated cyclopentane) were used as lubricants. In the mixed lubrication regime, approximately 0.007 to 0.2 m/s for the contacts studied here, the COF is dependent upon the ball material, speed, and precise amount of oil in the contact, and can vary from as low as 0.02 to as high as 0.16. The COF is lowest for the steel balls, higher for the silicon-nitride ball, and highest for the TiC-coated ball. The mixed lubrication regime is generally believed to consist of a combination of hydrodynamic and boundary lubrication; the relative amounts of boundary and hydrodynamic friction will vary with speed and lubricant amount, and the value of the boundary friction will vary with ball material. In the hydrodynamic regime (approximately 0.2 to 1 m/s in these experiments), the ball material no longer affects the COF since there are few asperity contacts to contribute boundary friction due to the increased entrainment of oil into the contact at these higher speeds. The two synthetic oils exhibit lower COF than the mineral oil in the hydrodynamic regime, a property that is generally referred to as improved "oiliness." The COF measured in these experiments increases proportionally with the square root of speed, as expected for hydrodynamic lubrication, with the synthetic oils about 0.01 to 0.02 lower in COF than the mineral oil. In the high-speed regime (above 1 m/s in these experiments), the COF no longer increases as rapidly as in the hydrodynamic region. Thermal effects and lubricant starvation are probably the causes of this behavior. The ball temperature near the contact was measured and found to be higher at higher speeds; this will decrease the viscosity of the oil and lower the hydrodynamic friction. In addition, as speed increases, the measured amount of oil on the ball decreases due to centrifugal force driving oil away from the ball surfaces farthest from the rotational axis. Less lubricant in the contact leads to lower hydrodynamic friction, but also to increased asperity contact and boundary friction. The interaction between these factors is complex, and the observed result is a lower COF at high speeds than expected if these factors are ignored. The data are provided in an appendix for use in modeling programs.

References

1. P. A. Bertrand, "Coefficient of Friction of a Lubricated Contact between Steel or Silicon Nitride Balls and Oil-Impregnated Cotton-Phenolic Material," TOR-2000(9975)-2, 20 December 1999.
2. P. A. Bertrand and J. D. Sinsheimer, "Humidity-Induced Dimensional Changes in Cotton-Phenolic Ball-Bearing Retainers," *Trans ASME* **124**, 474–479 (2002).
3. R. Stribeck, "Die Wesentlichen Eigenschaften der Gleit und Rollenlager," *Z. Ver. dt. Ing.* **46** (38), 1341–8, 1432–8 (1902); **46** (39), 1463–70 (1902).
4. S. Bair, P. Vergne, and M. Marchetti, "The Effect of Shear-Thinning on Film Thickness for Space Lubricants," *Tribol. Trans.* **45** (3), 330–333 (2002).
5. D. Nelias, E. Legrand, P. Vergne, and J.-B. Mondien, "Traction Behavior of Some Lubricants Used for Rolling Bearings in Spacecraft Applications: Experiments and Thermal Model Based on Primary Laboratory Data," *Trans. ASME* **124**, 72–81 (2002).
6. B. J. Hamrock and D. Dowson, *Ball Bearing Lubrication*, John Wiley & Sons, New York, 1981.
7. A. Cameron, *The Principles of Lubrication*, John Wiley & Sons, New York, 1966.
8. B. Ono and Y. Yamamoto, "Possibility of Slip in Hydrodynamic Oil Films Under Sliding Contact Conditions," *Lubric. Sci.* **14** (3), 303–320 (2002).
9. D. Zhu and Y.-Z. Hu, "A Computer Program Package for the Prediction of EHL and Mixed Lubrication Characteristics, Friction, Subsurface Stress and Flash Temperatures Based on Measured 3-D Surface Roughness," *Tribol. Trans.* **44** (3), 383–390 (2001); D. Zhu and Y.-Z. Hu, "Effects of Rough Surface Topography and Orientation on the Characteristics of EHD and Mixed Lubrication in both Circular and Elliptical Contacts," *Tribol. Trans.* **44** (3), 391–398 (2001); D. Zhu, "Effect of Surface Roughness on Mixed EHD Lubrication Characteristics," *Tribol. Trans.* **46** (1), 44–48 (2003).
10. M. D. Hersey, *Theory and Research in Lubrication*, John Wiley & Sons, New York, 1966.
11. H.-S. Chang and H. A. Spikes, "The Shear Stress Properties of Ester Lubricants in Elastohydrodynamic Contacts," *J. Synth. Lubric.* **9**, 91–114 (1992); M. Ratoi, V. Anghel, C. Bovington, and H. A. Spikes, "Mechanisms of oiliness additives," *Tribol. Int.* **33**, 241–247 (2000).
12. E. Höglund, "Influence of lubricant properties on elastohydrodynamic lubrication," *Wear* **232**, 176–184 (1999).

13. R. Khare, J. de Pablo, and A. Yethiraj, "Molecular simulation and continuum mechanics investigation of viscoelastic properties of fluids confined to molecularly thin films," *J. Chem. Phys.* **114** (17), 7593–7601 (2001); L. I. Kioupis and E. J. Maginn, "Impact of Molecular Architecture on the High-Pressure Rheology of Hydrocarbon Fluids," *J. Phys. Chem. B* **104**, 7774–7783 (2000).
14. D. Fuhrmann, A. P. Graham, L. Criswell, H. Mo, B. Matties, K. W. Herwig, and H. Taub, "Effects of chain branching on the monolayer structure of alkanes at interfaces: a neutron and helium atom scattering study," *Surf. Sci.* **482-485**, 77–82 (2001).
15. T. Toshiyuki and H. Hitoshi, "The fundamental molecular structure of synthetic traction fluids," *Tribol. Int.* **27** (3), 183–187 (1994).
16. M. Smeeth and H. A. Spikes, "The Influence of Slide/Roll Ratio on the Film Thickness of an EHD Contact Operating Within the Mixed Lubrication Regime," in *The Third Body Concept*, D. Dowson et al. (Editors), Elsevier Science B. V., 695–703 (1996).
17. C. R. Gentle and M. Pasdari, "Measurement of Cage and Pocket Friction in a Ball Bearing for Use in a Simulation Program," ASLE Preprint No. 84-LC-3C-1, 1984.
18. Y. P. Chiu, "An Analysis and Prediction of Lubricant Film Starvation in Rolling Contact Systems," *ASLE Trans.* **17** (1), 22–35 (1974).
19. F. Chevalier, A. A. Lubrecht, P. M. E. Cann, F. Colin and G. Dalmaz, "Starved Film Thickness: a Qualitative Explanation," in *Lubricants and Lubrication*, D. Dowson et al. (Editors), Elsevier Science B. V. 249–257 (1995).
20. A. Jabbarzadeh, J. D. Atkinson, and R. I. Tanner, "Effect of wall roughness on slip and rheological properties of hexadecane in molecular dynamics simulation of Couette shear flow between two sinusoidal walls," *Phys. Rev. E* **61** (1), 690–699 (2000).
21. S. Richardson, *J. Fluid Mech.* **59**, 707–719 (1973).

Appendix—COF Data

Table A-1. 0.875 in. (2.22 cm) Diameter 440C Steel Ball, “Well-Lubricated Conditions*”

Speed (m/s)	Apiezon C	Nye 2001	Nye 188B
0.012	0.062	0.024	0.072
0.036	0.045	0.018	0.056
0.060	0.036	0.018	0.048
0.12	0.037	0.020	0.040
0.24	0.040	0.036	0.055
0.42	0.078	0.062	0.076
0.6	0.111	0.085	0.092
1.2	0.136	0.114	0.104
1.8	0.162	0.148	0.126
6.1	0.165	0.162	0.167
7.6	0.152	0.160	0.161
9.0	0.139	0.150	0.150

Table A-2. 0.875 in. (2.22 cm) Diameter 440C Steel Ball, “Poorly Lubricated Conditions†”

Speed (m/s)	Apiezon C	Nye 2001	Nye 188B
0.012	0.086	0.057	0.066
0.036	0.096	0.088	0.077
0.060	0.110	0.090	0.084
0.12	0.132	0.109	0.100
0.24	0.154	0.129	0.132
0.42	0.170	0.157	0.158
0.6	0.188	0.176	0.166
1.2	0.214	0.208	0.186
1.8	0.218	0.222	0.188
6.1	0.210	0.204	0.202
7.6	0.204	0.213	0.204
9.0	0.196	0.194	0.190

*Values ± 0.009 . See text for description of “well-lubricated conditions.”

† Values ± 0.009 . See text for description of “poorly lubricated conditions.”

Table A-3. 0.875 in (2.22 cm) Diameter Silicon-Nitride Ball, "Well Lubricated Conditions**"

Speed (m/s)	Apiezon C	Nye 2001	Nye 188B
0.012	0.087	0.092	0.083
0.036	0.078	0.085	0.072
0.060	0.070	0.074	0.072
0.12	0.070	0.072	0.061
0.24	0.070	0.074	0.062
0.42	0.083	0.070	0.071
0.6	0.106	0.082	0.077
1.2	0.132	0.114	0.128
1.8	0.132	0.119	0.143
6.1	0.172	0.168	0.182
7.6	0.168	0.158	0.178
9.0	0.119	0.143	0.122

Table A-4: 0.875 in (2.22 cm) Diameter Silicon-Nitride Ball, "Poorly Lubricated Conditions†"

Speed (m/s)	Apiezon C	Nye 2001	Nye 188B
0.012	0.084	0.086	0.075
0.036	0.090	0.094	0.076
0.060	0.106	0.098	0.090
0.12	0.121	0.100	0.105
0.24	0.132	0.120	0.122
0.42	0.146	0.133	0.134
0.6	0.158	0.148	0.140
1.2	0.178	0.174	0.150
1.8	0.190	0.177	0.160
6.1	0.236	0.206	0.246
7.6	0.233	0.205	0.230
9.0	0.187	0.167	0.232

* Values ± 0.009 . See text for description of "well-lubricated conditions."

† Values ± 0.009 . See text for description of "poorly lubricated conditions."

Table A-5. 0.5 in. (1.27 cm) Diameter 440C Steel Ball, "Well-Lubricated Conditions**"

Speed (m/s)	Apiezon C	Nye 2001	Nye 188B
0.0067	0.077	0.060	0.074
0.020	0.063	0.052	0.066
0.033	0.060	0.054	0.060
0.067	0.060	0.058	0.058
0.13	0.055	0.052	0.056
0.23	0.048	0.052	0.050
0.33	0.056	0.059	0.052
0.67	0.099	0.079	0.078
1.0	0.120	0.102	0.100
3.4	0.119	0.084	0.126
4.2	0.105	0.093	0.105
5.0	0.095	0.098	0.103

Table A-6. 0.5 in. (1.27 cm) Diameter 440C Steel Ball, "Poorly Lubricated Conditions†"

Speed (m/s)	Apiezon C	Nye 2001	Nye 188B
0.0067	0.066	0.076	0.074
0.020	0.070	0.080	0.070
0.033	0.074	0.087	0.076
0.067	0.082	0.109	0.084
0.13	0.090	0.128	0.098
0.23	0.106	0.144	0.108
0.33	0.122	0.155	0.118
0.67	0.138	0.191	0.139
1.0	0.152	0.218	0.148
3.4	nm	0.162	0.198
4.2	nm	0.170	0.160
5.0	nm	0.171	0.156

* Values ± 0.009 . See text for description of "well-lubricated conditions."

† Values ± 0.009 . See text for description of "poorly lubricated conditions." Nm indicates value not measurable, too high for test fixture.

Table A-7. 0.5 in. (1.27 cm) Diameter TiC-Coated Steel Ball, "Well-Lubricated Conditions*"

Speed (m/s)	Aplezon C	Nye 2001	Nye 188B
0.0067	0.142	0.095	0.110
0.020	0.124	0.082	0.102
0.033	0.113	0.084	0.098
0.067	0.091	0.078	0.076
0.13	0.070	0.079	0.058
0.23	0.067	0.072	0.058
0.33	0.082	0.062	0.071
0.67	0.112	0.092	0.088
1.0	0.140	0.116	0.110
3.4	0.148	0.128	0.123
4.2	0.150	0.118	0.122
5.0	0.136	0.123	0.117

Table A-8. 0.5 in. (1.27 cm) Diameter TiC-Coated Steel Ball, "Poorly Lubricated Conditions†"

Speed (m/s)	Aplezon C	Nye 2001	Nye 188B
0.0067	0.146	0.163	0.160
0.020	0.150	0.166	0.162
0.033	0.152	0.172	0.168
0.067	0.154	0.172	0.160
0.13	0.168	0.170	0.168
0.23	0.153	0.173	0.164
0.33	0.158	0.175	0.164
0.67	0.150	0.162	0.168
1.0	0.158	0.164	0.156
3.4	nm	0.231	nm
4.2	nm	0.236	nm
5.0	nm	0.264	nm

* Values ± 0.009 . See text for description of "well lubricated conditions."

† Values ± 0.009 . See text for description of "poorly lubricated conditions." Nm indicates value not measurable, too high for test fixture.

LABORATORY OPERATIONS

The Aerospace Corporation functions as an "architect-engineer" for national security programs, specializing in advanced military space systems. The Corporation's Laboratory Operations supports the effective and timely development and operation of national security systems through scientific research and the application of advanced technology. Vital to the success of the Corporation is the technical staff's wide-ranging expertise and its ability to stay abreast of new technological developments and program support issues associated with rapidly evolving space systems. Contributing capabilities are provided by these individual organizations:

Electronics and Photonics Laboratory: Microelectronics, VLSI reliability, failure analysis, solid-state device physics, compound semiconductors, radiation effects, infrared and CCD detector devices, data storage and display technologies; lasers and electro-optics, solid-state laser design, micro-optics, optical communications, and fiber-optic sensors; atomic frequency standards, applied laser spectroscopy, laser chemistry, atmospheric propagation and beam control, LIDAR/LADAR remote sensing; solar cell and array testing and evaluation, battery electrochemistry, battery testing and evaluation.

Space Materials Laboratory: Evaluation and characterizations of new materials and processing techniques: metals, alloys, ceramics, polymers, thin films, and composites; development of advanced deposition processes; nondestructive evaluation, component failure analysis and reliability; structural mechanics, fracture mechanics, and stress corrosion; analysis and evaluation of materials at cryogenic and elevated temperatures; launch vehicle fluid mechanics, heat transfer and flight dynamics; aerothermodynamics; chemical and electric propulsion; environmental chemistry; combustion processes; space environment effects on materials, hardening and vulnerability assessment; contamination, thermal and structural control; lubrication and surface phenomena. Microelectromechanical systems (MEMS) for space applications; laser micromachining; laser-surface physical and chemical interactions; micropropulsion; micro- and nanosatellite mission analysis; intelligent microinstruments for monitoring space and launch system environments.

Space Science Applications Laboratory: Magnetospheric, auroral and cosmic-ray physics, wave-particle interactions, magnetospheric plasma waves; atmospheric and ionospheric physics, density and composition of the upper atmosphere, remote sensing using atmospheric radiation; solar physics, infrared astronomy, infrared signature analysis; infrared surveillance, imaging and remote sensing; multispectral and hyperspectral sensor development; data analysis and algorithm development; applications of multispectral and hyperspectral imagery to defense, civil space, commercial, and environmental missions; effects of solar activity, magnetic storms and nuclear explosions on the Earth's atmosphere, ionosphere and magnetosphere; effects of electromagnetic and particulate radiations on space systems; space instrumentation, design, fabrication and test; environmental chemistry, trace detection; atmospheric chemical reactions, atmospheric optics, light scattering, state-specific chemical reactions, and radiative signatures of missile plumes.